

BEFORE THE UNITED STATES  
NUCLEAR REGULATORY COMMISSION

In the Matter of )  
 )  
POWER AUTHORITY OF THE )  
STATE OF NEW YORK )  
 )  
and )  
 )  
CONSOLIDATED EDISON COMPANY )  
OF NEW YORK, INC. )

DOCKET NO. 50-286

AMENDMENT NO. 2 to  
APPLICATION FOR AMENDMENT TO  
OPERATING LICENSE

On September 2, 1977 the Power Authority of the State of New York ("Power Authority"), as sole owner of the Indian Point 3 Nuclear Power Plant and co-holder of Facility Operating License No. DPR-64 (for which Consolidated Edison presently has operating responsibility as co-licensee) filed an application for amendment to Operating License No. DPR-64 for the purpose of amending portions of Technical Specification 3.8 set forth in Appendix A to that license and requesting the Commission to review a proposed modification to the Indian Point 3 Nuclear Power Plant.

The Power Authority hereby amends Attachment A of the above-mentioned application to include additional information as requested by the NRC Staff. This additional information is presented in Attachment I to this application, which is incorporated herein by reference.

POWER AUTHORITY OF THE  
STATE OF NEW YORK

By

*George T. Berry*  
George T. Berry  
General Manager and  
Chief Engineer

Subscribed and sworn to before  
me this 9th day of December, 1977

*Maureen A. Morris*  
Notary Public

8111050327 771212  
PDR ADOCK 05000286  
PDR

MAUREEN A. MORRIS  
Notary Public, State of New York  
No. 4528251  
Qualified in Kings County  
Commission Expires March 30, 1978

BEFORE THE UNITED STATES  
NUCLEAR REGULATORY COMMISSION

In the Matter of )  
 )  
POWER AUTHORITY OF THE )  
STATE OF NEW YORK )  
 )  
and ) Docket No. 50-286  
 )  
CONSOLIDATED EDISON COMPANY )  
OF NEW YORK, INC. )

CERTIFICATE OF SERVICE

I certify that I have, this 13th day of December, 1977, served the foregoing document entitled "Amendment No. 2 to Application for Amendment to Operating License," together with Attachment, dated December 8, 1977 by mailing copies thereof, first class postage prepaid and properly addressed to the following persons:

Hon. George V. Begany  
Mayor, Village of Buchanan  
188 Westchester Avenue  
Buchanan, New York 10511

Hendrick Hudson Free Library  
31 Albany Post Road  
Montrose, New York 10548

  
Lex K. Larson

LeBoeuf, Lamb, Leiby & MacRae  
Attorneys for Applicant

ATTACHMENT I

RESPONSES TO NOVEMBER 20, 1977 QUESTIONS BY NRC

Power Authority of the State of New York

1. Describe the qualification procedures for the material property values including yield strength, ultimate strength, and percent elongation used for the analysis of the boron-stainless steel plates attached to the sides of the fuel storage cells.

Response

The material property values of the boron-stainless steel plates were specified by the manufacturer, Carpenter Technology, on the Certified Material Test Reports. The material property values ranged as follows:

Yield Strength, ksi @ 0.2%	30.0-56.0
Ultimate Strength, ksi	79.5-90.0
Percent Elongation in 2",%	13.0-29.0

These values were determined, by Carpenter Technology, in accordance with ASME SA-370, "Mechanical Testing of Steel Products."

2. Describe and provide clear drawings of the locations and type of welds used to attach the boron-stainless steel plates to the sides of the fuel storage cells. Describe the procedures and qualifications used in performing these welds and discuss the effects of welding on the material properties requested in number 1.

### Response

The weld used to attach the boron-stainless steel plates to the sides of the fuel storage cells is a 1/8 inch fillet weld as shown on Figure 2.1.5. This is a skip weld, 1-1/2 inches on 12 inch centers.

The weld procedure, which will be used for this weld, will utilize the gas metal arc welding process (GMAW-S). This weld process was selected to minimize the heat input during welding in order to reduce the formation of a boron phase in the weld heat affected zone. ER-312 filler metal will be employed to ensure a high ferrite content in the weld metal and therefore, reduce the possibility of microfissuring caused by large or connecting boron phases. The weld procedure will be qualified as a fillet weld test of the production joint. The qualification will be run at the maximum and minimum heat inputs allowed by the procedure, and in the most restrictive joint position expected during production welding. The qualification will be in compliance with Regulatory Guide 1.71.

Preliminary testing has been performed on the production weld joint using the above described weld procedure. This testing involved ultimate tensile tests of the production weld joint (i.e., a fillet weld shear test which results in almost pure tension on the fusion surface of the boron-stainless steel). The ultimate tensile strength ranged from 36 to 51 ksi. All the test specimens failed at the fusion zone surface of the boron-stainless steel. Based on the allowable stress limits for ASME Section III, Subsection NF for linear component support welds, an allowable shear stress on a fillet weld (regardless of the direction of application of the load) can be derived by taking three tenths (0.3) of the ultimate strength. Using the minimum value of the ultimate strength range, the allowable fillet weld shear stress would be 10 ksi. No elongation data was accumulated during the testing.

3. Define the most critical loading combination and provide the corresponding highest stresses and strains and their locations in the boron-stainless steel plates. Consider in this analysis any thermal stresses induced due to different coefficients of thermal expansion in the boron-stainless steel plates and the stainless steel fuel cells. Compare these stresses and strains to the allowable stresses and strains based on the material values from 1 and 2.

#### Response

Deflection of the fuel cell during a seismic event applies a combined bending and compressive load on the boron-stainless steel plate. The OBE seismic condition is the most critical load combination on the plate and results in a stress of 5,600 PSI. This compares to an allowable of 16,500 PSI (based on the minimum yield strength listed in Item #1, and the design requirements of ASME Section III, NF-3400, for linear component supports). The same load combination creates a 4,200 PSI shear stress in the fillet weld attaching the plate to the fuel cell. This compares to an allowable fillet weld shear stress of 10,000 PSI as listed in Item #2. The fillet welds attaching the plates to the storage cells are sufficiently closely spaced to prevent buckling of the plates. The boron-stainless steel manufacturer lists the mean coefficient of thermal expansion for type 304 stainless steel as  $10.4 \times 10^{-6}$  in/in/°F and for the boron-stainless steel as  $10.5 \times 10^{-6}$  in/in/°F. These coefficients are so close that thermal stresses induced by their difference would be negligible.

It is concluded, that the stresses in the boron-stainless steel plates and their attachment welds are well within the allowable values established from the actual material test data.

4. Discuss the corrosion resistance of the boron-stainless steel plates.

#### Response

The discussion that follows is extracted from: "Corrosion in Nuclear Application" by Warren E. Berry, a volume in the Corrosion Monographs Series, edited by R.T. Foky, N. Hackerman, C.V. King, F.L. LaQue, H.H. Uhlig, and Z.A. Foroulis, published by J. Wiley & Sons, Inc., 1971.

Boron stainless steels containing up to 2.5 wt percent boron corrode at about the same, or somewhat higher rates than comparable alloys without boron. There are indications that corrosion increases with increasing boron in the alloy and with increasing exposure time. Data for exposure of boron stainless steel to static water are summarized in Table 4.1. Dynamic tests at 12 ft/s in 260 C water reveal average corrosion rates of less than 4 mg/dm<sup>2</sup> month for 1.2 and 1.6 wt percent boron stainless steels.

Boron stainless steel dispersions in stainless steel corrode at the exposed boride until it and the surrounding reacted area of stainless steel are corroded away. The corrosion rate then decreases to a low level, commensurate with that of the base material. Stainless steel containing 4 vol. percent boron carbide dispersion exhibits weight gains of 62 to 73 mg/dm<sup>2</sup> after 14 day exposure in 360 C water.

Note that maximum fuel pool water design temperature will not exceed 66 C, in contrast with temperatures of 260 C and 360 C indicated above, with water flows of less than 1 ft/s.

Table 4.1 - STATIC WATER CORROSION TEST OF BORON STAINLESS STEEL cont'd

Ni	B	B	C	Condition	Time hr.	Average weight change mg/dm <sup>2</sup>	Comments
14	2.8	NA	288	Degassed	3,161	+12.5	As cast
14	2.8	NA	288	Degassed	3,161	+ 8.0	As cast Adherent dull
14	2.2	NA	288	Degassed	3,161	-14.9	Ht.tr. 1236C for 3 hr. black coating
14	2.2	NA	288	Degassed	3,161	-0.4	Ht.tr. 1236C for 3 hr.
7	12.2	4.	288	Degassed	633	-26.0	Slightly loose, uneven, brown- black coating
7	12.2	4.	288	Air-satd.	633	+20.3	Adherent black coating

Table 4.1 - STATIC WATER CORROSION TEST OF BORON STAINLESS STEEL

Nominal composition wt percent			Analyzed wt percent	Temp. C	Condition	Time hr.	Average weight change mg/dm <sup>2</sup>	Comments
Ni	B		B					
3	11	1	0.96, 1.01	288	Degassed	2,517	-6.2	Adherent brown-black coating
3	11	1	0.96, 1.01	288	Air-satd.	2,517	-9.5	Adherent black coating
3.8	8.7	2	1.85	288	Degassed	1,908	+12.5	Adherent black coating. Areas where samples are in contact are noticeable
3.8	8.7	2	1.85	288	Air-satd.	1,908	+21.4	Adherent brown and black coating Loose black coating where samples are in contact. Dark tarnish spot at one end.
3.8	8.7	2	1.96	288	Degassed	1,032	+13.3	Adherent black coating
3.8	8.7	2	1.96	288	Air-satd.	1,032	+11.3	Adherent blue-black to brown-black tarnish
1	14.8	1	1.16	288	Degassed	663	+3.2	Adherent brown, red-brown, purple and black tarnish
	14.8	1	1.16	288	Air-satd.	663	+1.6	Adherent brown to black tarnish
	8	1	NA (a)	316	Degassed	3,538	+5	Adherent black coating
	8	1	NA	316	Air-satd.	3,538	+7.9	Adherent brown-black tarnish
	8	1	NA	316	Degassed	3,538	+11.3	Pickled before test in 40 percent HNO <sub>3</sub> , 4 percent HF. Adherent black coating
	8	2	NA	316	Degassed	3,538	+5	Adherent black coating
	8	2	NA	316	Air-satd.	3,538	-18.9	Adherent grey-black coating
	8	2	NA	316	Degassed	3,538	+2.5	Pickled before test in 40 percent HNO <sub>3</sub> 4 percent HF. Adherent blue-black coating
	8	3	NA	316	Degassed	3,538	-1.2	Adherent black coating
	8	3	NA	316	Air-satd.	3,538	+11.4	Adherent black coating
	8	3	NA	316	Degassed	3,538	-99.9	Pickled before test in 40 percent HNO <sub>3</sub> , 4 percent HF. Adherent blue-black coating

5. Describe how the individual fuel assembly to fuel cell impacts were summed to determine their contribution to the rack to rack and rack to pool wall reaction forces.

Response

As described in Section 2.1.4 of the September 1, 1977 detailed submittal, the nonlinear analysis of the fuel cell/fuel assembly resulted in loads equal to only 52% of the loads calculated by the linear elastic time history analysis. It was therefore, concluded that application of the fuel storage cell/fuel assembly lumped mass modeling assumption in the complete rack module linear elastic analysis with an impact factor of unity would be a conservative and acceptable procedure. This same conservative procedure was used to determine the rack-to-rack and rack-to-pool reactor forces. The contribution of the fuel to the seismic loads, within the racks and on the interties and pool structure was, therefore, conservatively accounted for.

6. Describe the extent to which interaction between storage racks was analyzed including a clear description of the rack to rack interties and the boundary condition used to model the interties.

Response

Details of the rack intertie design are shown in Figure 2.1.6. Three (3) such interties are provided at all rack-to-rack interfaces. The interties are designed to permit relative horizontal movement between racks to accommodate thermal expansion. Rack overturning under seismic conditions is prevented by transmission of vertical shear forces from rack-to-rack. The minimum requirement for seismic stability is two (2) racks, intertied at their common boundary. This condition occurs in the North-South direction at Racks B-4 and B-5 shown on Figure 2.0.2 Revision 1, attached. This is the configuration which was modeled in the seismic analysis. Figure 2.1.1 (Revision 1) shows the boundary conditions applied to the seismic model at the rack interties.

7. Discuss the integrity of the fuel assemblies inside the fuel racks during a seismic event, including a comparison of maximum to allowable stresses.

Response

During a seismic event the top end fitting and the intermediate spacer grids of the fuel assemblies experience maximum loads of 1680 lbs and 700 lbs, respectively. It is anticipated that these loads are significantly lower than the allowables for the fuel assembly.

8. Provide clearer sketches of the rack feet and pool floor embedments which in combination with friction are relied upon to resist horizontal seismic loads. Discuss the possibility and effects of sliding of racks on the pool floor.

Response

Details of the screw adjustable rack feet and attachment of the racks to the existing embedments are shown in Figure 2.1.7. The existing embedments consist of lengths of 4" (4.5" O.D.), schedule 40 pipe welded to the pool floor liner plate. The allowable shear loads on each embedment are 29,100 lbs and 46,600 lbs for OBE and SSE loadings respectively.

Loads are transmitted from the rack structure to the embedments by adaptor plates welded to the bases of the racks. Horizontal seismic loads are resisted by the existing embedments and frictional forces on the rack feet working in combination.

At the maximum allowable load on the existing embedments, the minimum friction coefficients, required to resist the horizontal seismic loads, are 0.23 and 0.29 for OBE and SSE loadings, respectively. The reference\* provides details of a variety of friction tests representative of water reactor operating conditions. For a Type 304 stainless steel sliding couple, the following friction coefficients were measured.

<u>Experiment</u>	<u>Lubrication</u>	<u>Friction Coefficient</u>	
		<u>100 psi</u>	<u>1,500 psi</u>
304 SS on 304 SS	Dry at 74°F	0.40	0.44
304 SS on 304 SS	Water at 200°F	0.59	0.48

The actual operating condition is at approximately 120°F and an average bearing pressure of 440 psi at which conditions a sliding coefficient of friction of a least 0.45 would be anticipated. The static friction coefficient would be expected to be even higher. It is concluded, therefore, that there is a margin of at least 50% against sliding of the racks on the pool floor.

Detailed nonlinear time history analyses have been performed to investigate the sliding behavior of a similar rack design. The analysis was performed for a seismic response spectrum which completely enveloped the Indian Point 3 spectrum. Based on this analysis at a friction coefficient of only 0.2 and taking no credit for restraint by the embedments, it is expected that the maximum rack movement on the pool floor would not exceed 0.1 inches. There would, therefore, be no significant consequence of rack sliding under this extremely unlikely set of conditions.

\*REFERENCE: General Electric Report No. 60GL20, "Investigation of the Sliding Behavior of a Number of Alloys Under Dry and Water Lubricated Conditions", R. E. Lee, Jr., January 22, 1960.

9. Describe the restraints at the top of the racks on the north-east fuel pool wall and any additional gaps between the racks and the fuel pool wall. Discuss the possibility of impacting at these gaps due to possible seismic response, including sliding, and discuss the effects of the impact on the fuel rack and the fuel pool wall.

#### Response

Details of the upper wall restraints on Rack A-1 in the North-East corner of the pool are shown in Figure 2.1.8. The restraints are bolted to the upper peripheral frame members of the racks and will be adjusted at installation to provide a 1/16" thermal expansion gap. The maximum calculated load on these restraints under SSE loading conditions is 9.85 kips. This load was increased by a factor of 2.0 to 19.7 kips to allow for impact effects resulting from the clearance of approximately 1/32" at normal operating temperature. The maximum allowable load on the restraint and the rack structure is 21.1 kips. The pool wall is capable of resisting a continuous line load of 50.0 kips/ft at the elevation of the restraints. The applied load of 19.7 kips is, therefore, well within the capacity of the pool wall.

10. Justify the adequacy of the fuel pool structure to withstand the thermal stresses due to the increase in the maximum design basis transient temperature due to the increase in fuel pool storage capacity.

Response

The fuel pool structure was evaluated to determine its ability to withstand the thermal effects due to the increase in maximum design basis transient temperatures. The operating thermal gradient and the abnormal condition thermal gradient were assumed as 150°F and 212°F respectively. The effect of the gradients was determined in accordance with ACI-207-69 Specification for the Design and Construction of Reinforced Concrete Chimneys. The thermal effects were added to the dead loads, hydrostatic loads and seismic loads in accordance with the load combinations in the US NRC Standard Review Plan Section 3.8.4. The capacity of the structure was found adequate to resist the combined loads and thermal effects within the Structural Acceptance Criteria of SRP 3.8.4.

11. In reference to a dropped fuel assembly accident, describe what portion of the fuel storage cell above the stored fuel assembly is relied upon to absorb the energy of a dropped fuel assembly.

Response

Figure 2.1.9 shows the arrangement of the fuel cell with respect to the top grid structure of the rack and a stored fuel assembly. The 8" of fuel cell protruding above the top grid is relied upon to absorb the energy of a dropped fuel assembly. The impact is primarily absorbed by local crushing of the top 2 to 3 inches of the cell, above the stored fuel. The maximum deflection of the top of the cell is approximately one (1) inch.

12. Discuss any testing or inservice surveillance programs conducted or planned to verify long term material stability and mechanical integrity of the fuel storage rack elements.

Response

All fuel storage rack elements, with the exception of the borated stainless steel plates discussed in question 4, are constructed of Type 304 stainless steel. Experience gained through the utilization of Type 304 stainless steel for this application has demonstrated the capability of this material to maintain long term material stability and mechanical integrity under the operating conditions proposed.

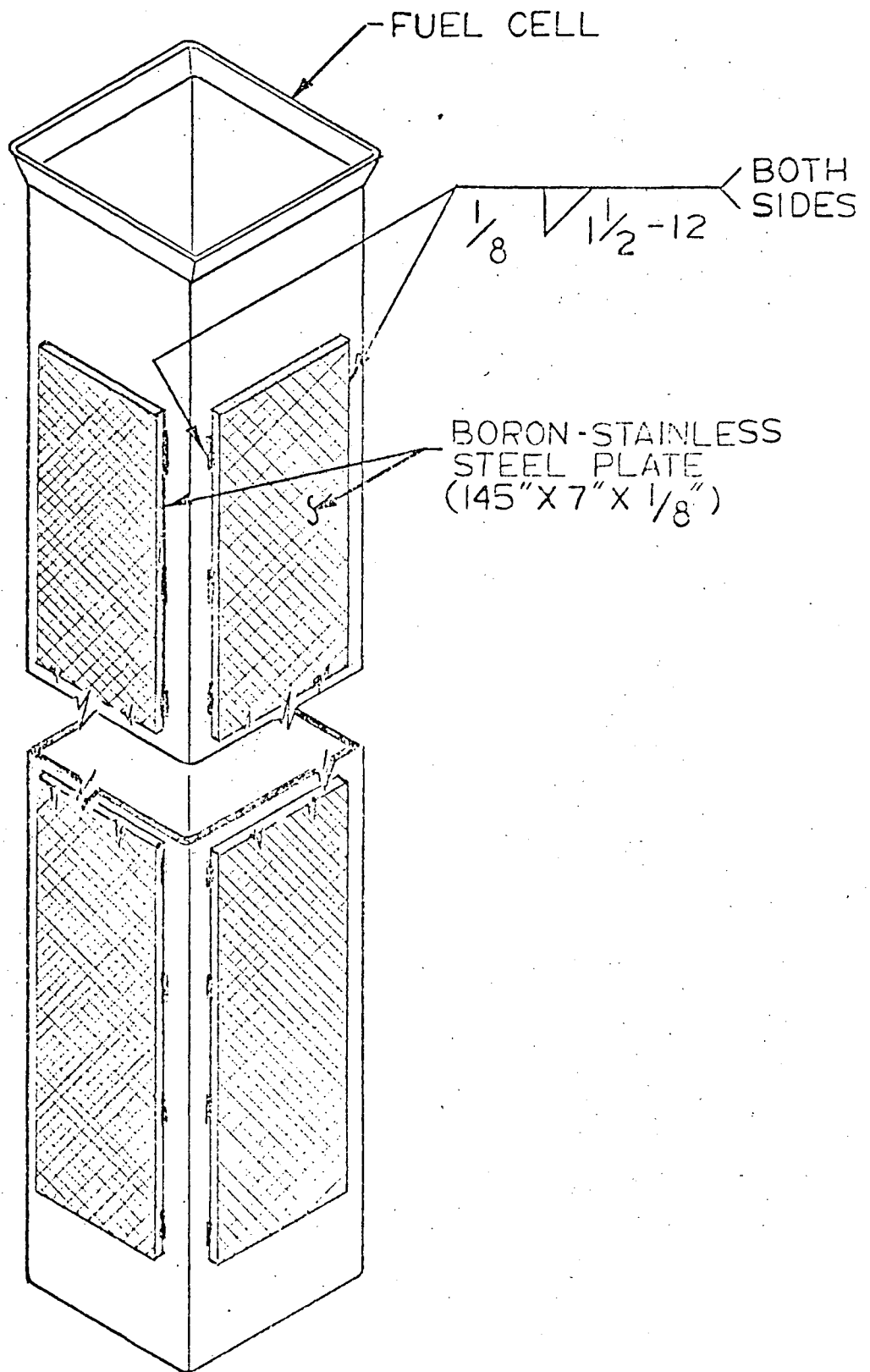


FIGURE 2.1.5

Boron-Stainless Steel Plate Attachment

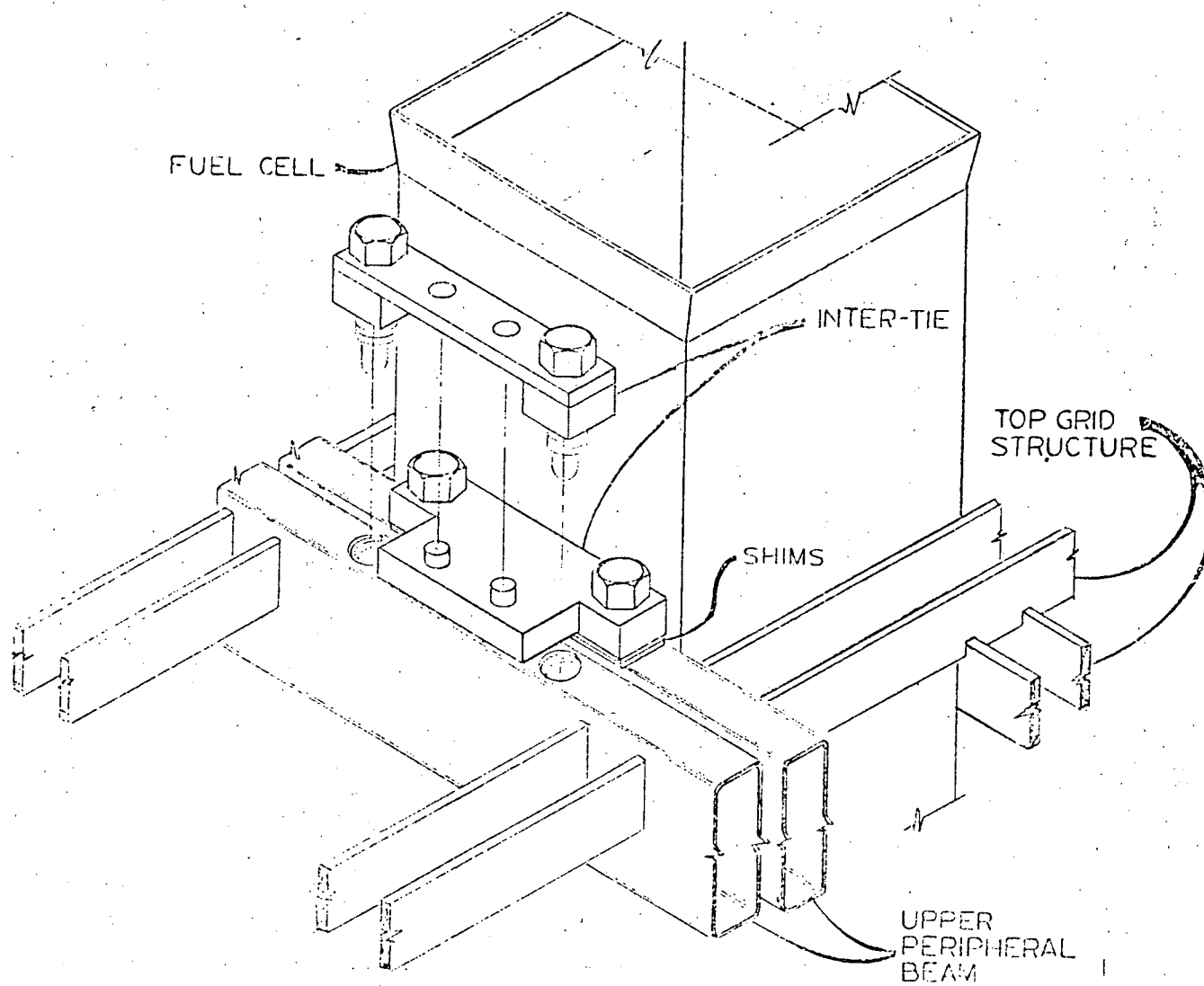


FIGURE 2.1.6 Rack Interties

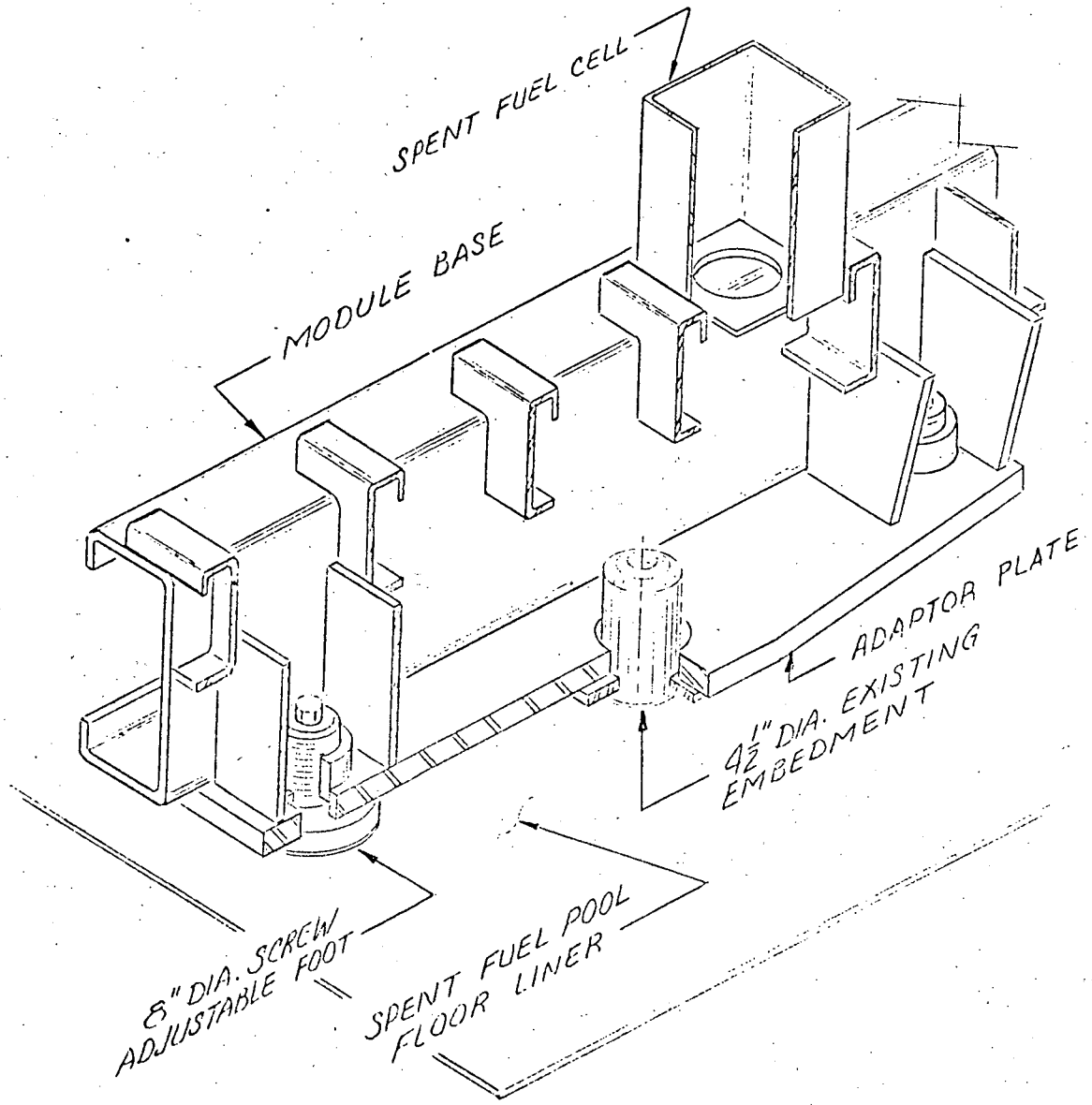


FIGURE 2.1.7 Rack Base and Embedment Details

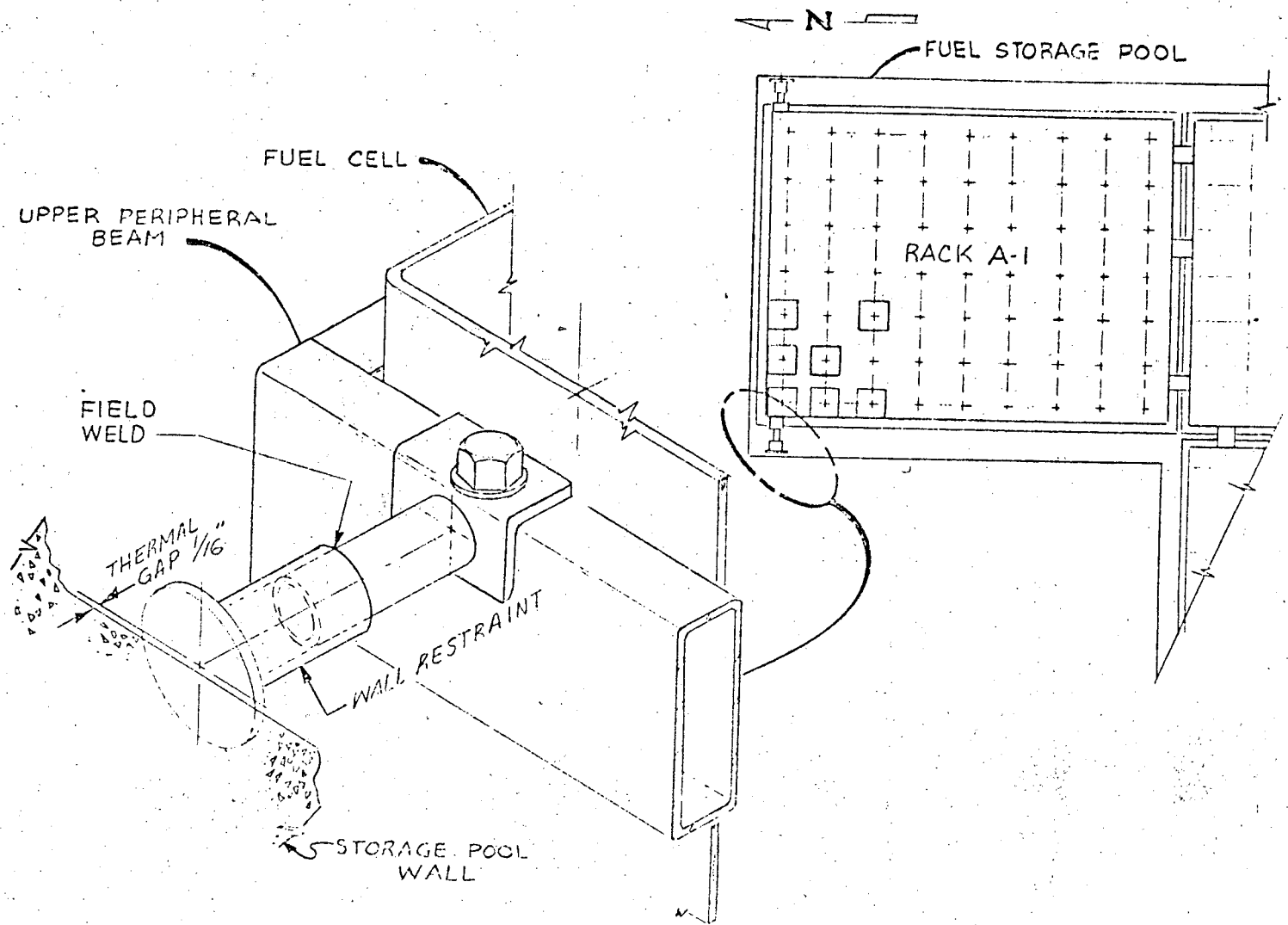


FIGURE 2.1.8 Rack A-1 Upper Wall Restraint

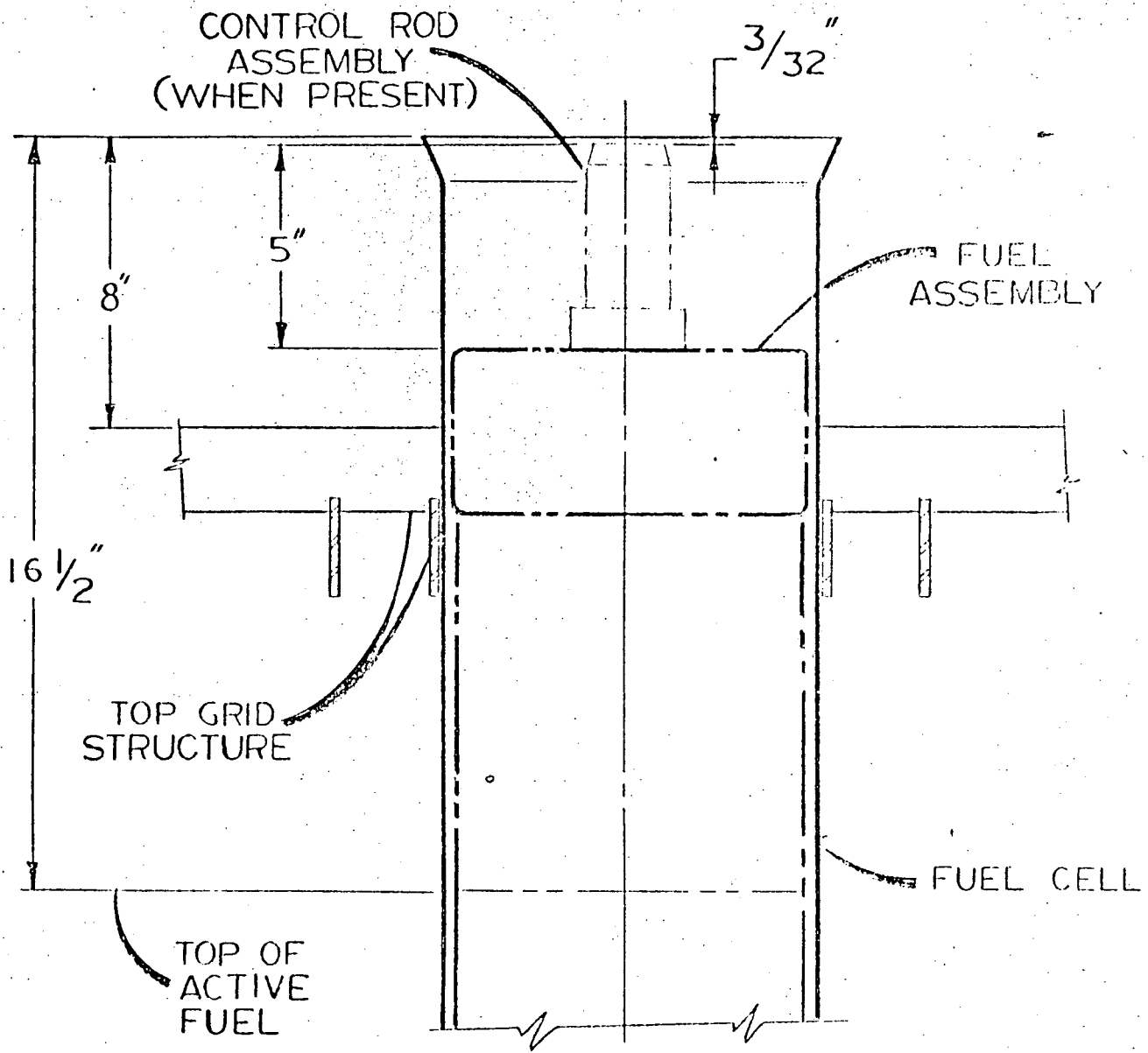
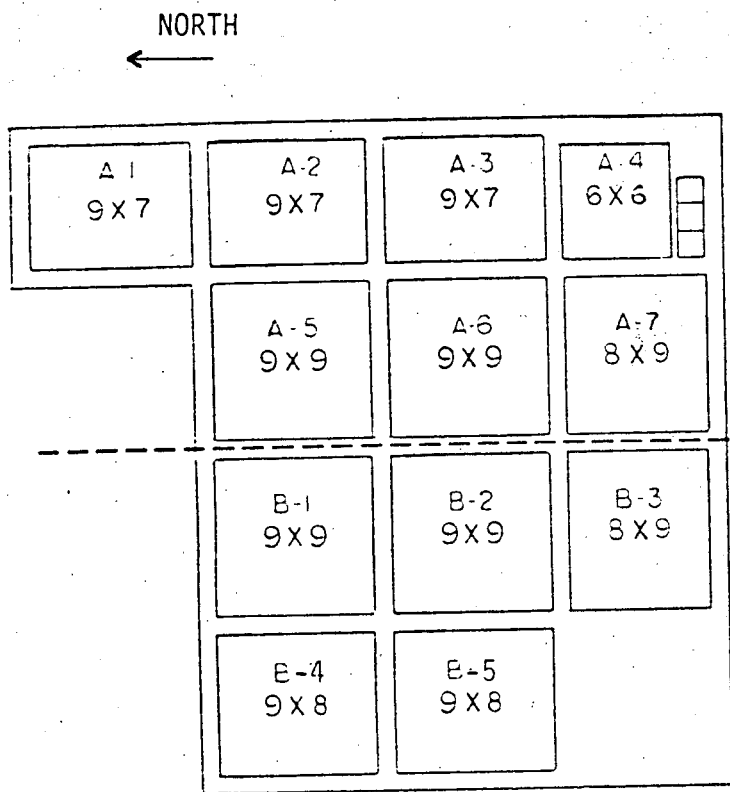


FIGURE 2.1.9 Detail At Top Of Fuel Storage Cell

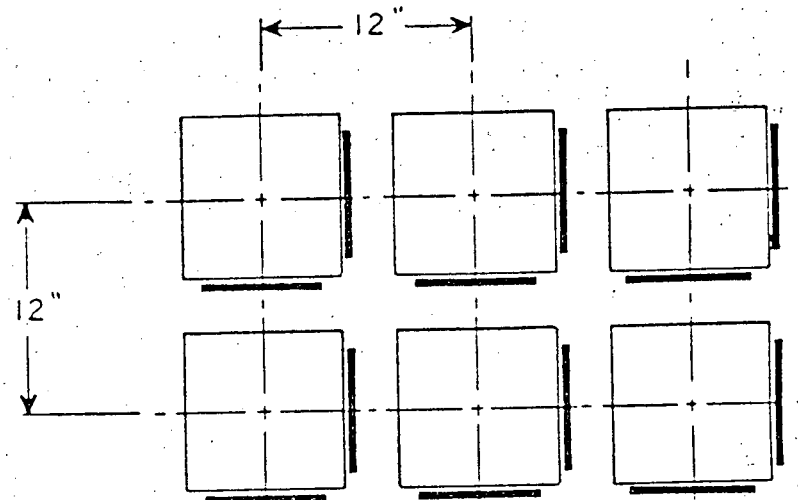


PLAN-GENERAL ARRANGEMENT

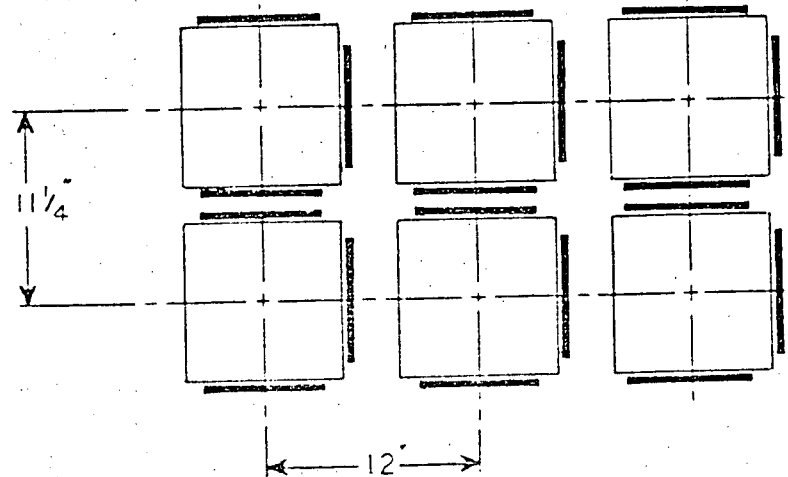
TOTAL SPENT FUEL STORAGE CAPACITY, 837 POSITIONS  
 TOTAL FAILED FUEL STORAGE CAPACITY 3 POSITIONS

INDIAN POINT UNIT No 3

A AREA  
-----  
B AREA



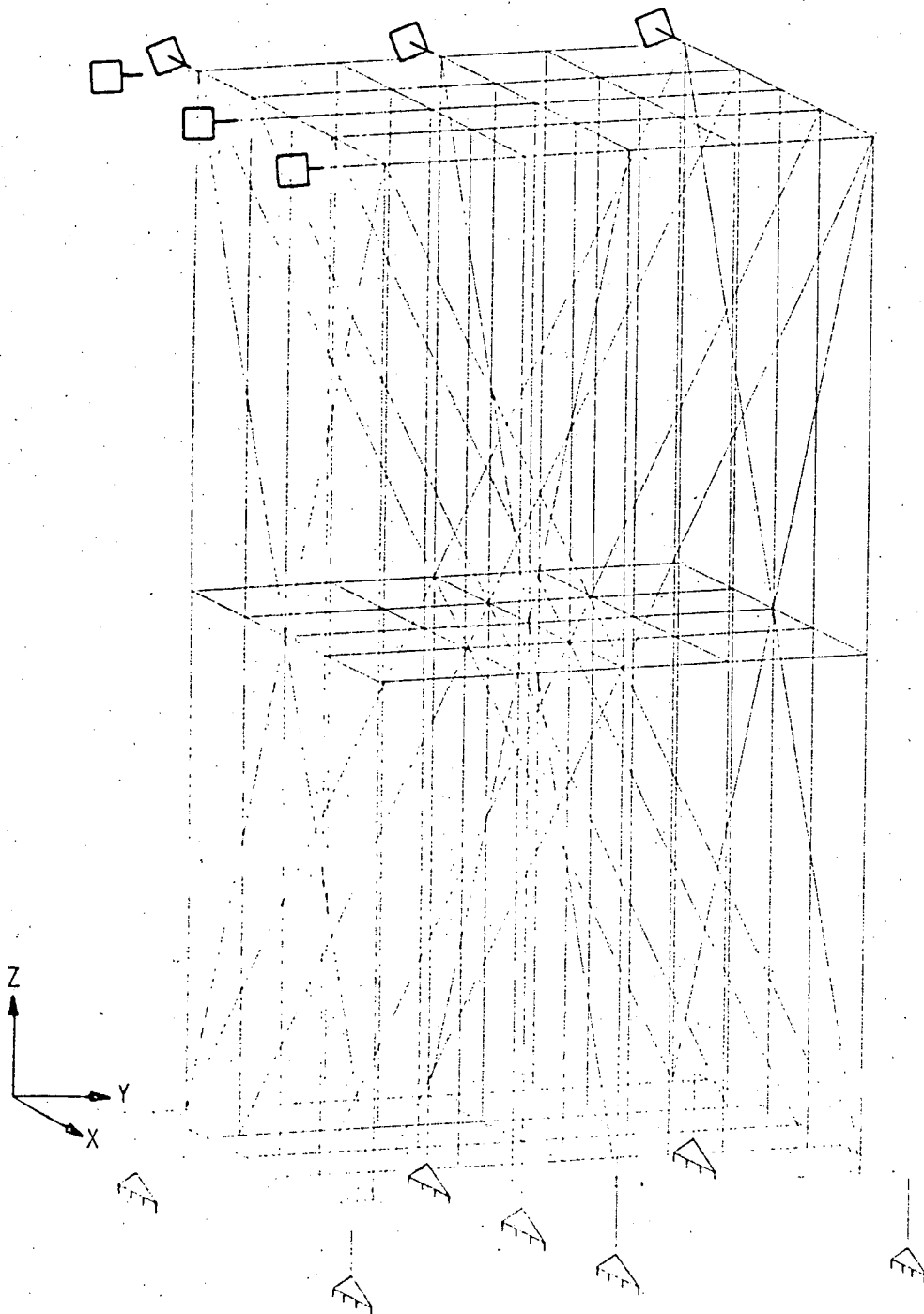
UPPER SECTION = 805 PLATES



LOWER SECTION = 1003 PLATES

TOTAL PLATES, 1808

FIGURE 2.0.2  
(REVISION 1)



Legend - Boundary Conditions at  
rack inertias

□  $\delta z = 0$  for Y-Direction  
seismic loads, free for  
X and Z loading.

◇  $\delta z = 0$  for X-Direction  
seismic loads, free for  
Y and Z loading.

SEISMIC MODEL

FIGURE 2.1.1 (Rev. 1)